Temperature and magnetism of gray optical lattices

K. I. Petsas, J.-Y. Courtois,* and G. Grynberg
Laboratoire Kastler-Brossel, Département de Physique de l'Ecole Normale Supérieure, 24 rue Lhomond, F-75231 Paris Cedex 05, France
(Received 5 July 1995)

We present a theoretical investigation of the temperature and of the magnetization of atoms in one-dimensional ''gray'' optical lattices. Such lattices consist of counterpropagating beams having crossed linear polarizations, tuned on the blue side of a $J \rightarrow J$ or a $J \rightarrow J-1$ transition, and a static longitudinal magnetic field. The variation of the atomic temperature with the magnetic field recently observed (an increase at low magnetic field; a decrease towards an asymptotic value at high magnetic field) is found for any atomic transition admitting one or two uncoupled states. This change of behavior of the temperature results from a qualitative change of the cooling mechanism and is correlated with a transition from paramagnetism to antiparamagnetism in the optical lattice.

PACS number(s): 32.80.Pj

The outstanding development of laser cooling and trapping of neutral atoms originates from the pioneering proposal by Hänsch and Schawlow [1] about Doppler cooling. But it would certainly never have attracted so much attention without the experimental discovery [2] and theoretical interpretation [3] of the so-called sub-Doppler cooling mechanisms, the best known of which is Sisyphus cooling. One of the most striking features of this cooling mechanism is the possibility for atoms to be efficiently and durably trapped in the optical potential wells associated with the light shifts [4], where they undergo an oscillating motion. The experimental observation of this vibrational motion is possible because of the strong spatial confinement of the atoms on the wavelength scale (Lamb-Dicke regime), which yields a narrowing of the atomic vibrational levels [5]. It was first achieved in one-dimensional (1D) [6,7] and then in 2D [8] geometries using stimulated or spontaneous Raman spectroscopy. Finally, the experimental demonstration of atom localization in a 3D lattice of micrometer-sized optical potential wells [9–11] was a major achievement in the field of laser cooling, from which emerged the new field of ''optical lattices.''

All these early experiments were realized by tuning the lattice beams on the red side of an atomic transition connecting the ground state of angular momentum J_g to an excited state of larger angular momentum $J_e = J_g + 1$. In such lattices, atoms are trapped at locations where their interaction with the trapping beams is maximum and therefore scatter a large number of photons from the trapping field. This is why Rayleigh scattering is the main feature of the fluorescence spectrum of these ''bright'' lattices [7] (the fact that *elastic* scattering dominates the spectrum is due to the Lamb-Dicke effect [5]). This also implies that bright lattices are characterized by strong atom-atom interactions, resulting in particular from transfers of momentum between atoms via reabsorption of scattered photons, and therefore by a small filling factor of the potential wells.

It was thus realized that another type of lattice was needed, where atoms would be trapped near points where their interaction with light would be minimum. We recently proposed one possible scheme for realizing such a lattice [12]. It is analogous to the so-called lin $\perp$ lin [3] bright lattice, except that the angular momentum of the ground state is either equal to ($J_e = J_g$) or larger ($J_e = J_g - 1$) than that of the excited state and that the laser beams are tuned on the blue side of the atomic transition. The peculiarity of such configurations is the existence, at any point in space, of at least one internal state being decoupled from light. These ''uncoupled'' (or ''nearly dark'') states experience no light shift and lead to a flat optical potential, where atoms tend to accumulate as a result of the very small departure rate from the uncoupled potential. This leads to an efficient cooling mechanism, as well as to a significant reduction of photon scattering from the atoms, as recently demonstrated experimentally in 3D four-beam molasses geometries [13]. To further obtain an efficient spatial localization, a static longitudinal magnetic field should be used, as proposed theoretically in [12] and studied recently in [14]. One of the most striking properties of the resulting ''gray'' four-beam lattices revealed by the experiment is the variation of the atomic temperature with the magnitude of the static magnetic field [15]. It was observed that the temperature increases with the magnetic field as long as the Zeeman splitting $\hbar\Omega_B$ between the outermost ground-state Zeeman sublevels is smaller than the typical light shift $\hbar\Delta'$ of the coupled states, reaches its maximum when $\hbar\Omega_B$ is of the order of $\hbar\Delta'$, and then decreases towards an asymptotic value. We show in this paper that such a behavior already arises in one dimension for any transition involving uncoupled states and that the asymptotic temperature reached in the limit of large magnetic field is a linear function of $\hbar\Delta'$ on a large range of parameters. The magnetization of these gray lattices, which is a quantity accessible to experiments, is also considered. We find in particular that the lattice magnetization exhibits a behavior analogous to that of the atomic temperature: increase in the limit of small magnetic field (paramagnetic behavior), then decrease down to zero in the large field limit (antiparamagnetic behavior). We show that these observations result from a qualita

*Permanent address: Institut d'Optique Théorique et Appliquée, B.P. 147, F-91403 Orsay Cedex, France.

tive change of cooling mechanism in the lattice. Finally, the characteristics and predictions of our 1D model are compared to the geometry and results of a recent experiment [15] using a 3D stretched tetrahedron [16].

Consider an atomic ensemble interacting with two linearly cross-polarized counterpropagating laser beams and a static magnetic field aligned along their propagation axis Oz. Both lasers have the same amplitude and frequency ω and are tuned on the blue side of a closed transition connecting the atomic ground state of angular momentum J_g to an excited state of angular momentum $J_e=J_g$ or J_g-1 [the frequency detuning $\Delta=\omega-\omega_A$ between the lasers (ω) and the atomic resonance frequency (ω_A) is positive]. The combined effect of the light and magnetic fields results in space-dependent energy shifts of the ground-state Zeeman sublevels, which act as external potentials for the atomic center-of-mass degrees of freedom. The actual shape of these optical potentials, which underlies the properties of the lattice, depends on the relative magnitude of the typical light shift $\hbar\Delta'=\hbar\Omega^2/2\Delta$ (Ω is the resonant Rabi frequency corresponding to one laser beam and a Clebsch-Gordan coefficient equal to 1) and of the Zeeman splitting $\hbar\Omega_B$ between the outermost ground-state sublevels $|+J_g\rangle$ and $|-J_g\rangle$ (in the absence of the laser field). In particular, two simple limiting regimes can be readily characterized. In the case $\Omega_B \ll \Delta'$, where the Zeeman splitting is a small perturbation compared to the light shifts, the lowest optical potential is mainly associated with the uncoupled states. Because of the nonzero magnetic field, this potential exhibits a spatial modulation arising from an admixture of the Zeeman shifts of the space-dependent uncoupled states. As shown theoretically in [12], atoms are localized in the wells of this potential, where they very weakly interact with light. By contrast, in the limit $\Omega_B \gg \Delta'$, where the light shifts are a small perturbation compared to the Zeeman splitting, the optical potentials are essentially associated with the bare ground-state Zeeman sublevels $|m_g\rangle$. These potentials are spatially modulated because of the light shifts induced by the space-dependent laser field. In particular, the two outermost optical potentials (associated with the $|+J_g\rangle$ and $|-J_g\rangle$ states) exhibit minima at points where the Zeeman sublevels coincide with the uncoupled state. One therefore expects atoms to accumulate at the bottom of these potentials, hence minimizing their interaction with light.

In the following, we denote by low magnetic-field regime the regime where the potential curves originating from the uncoupled states are well separated from the other potential curves. The typical range for the low-field limit is $\Omega_B < \Omega_l$, where Ω_l is the value for which a crossing occurs between the lowest potential curve and a potential curve associated with a coupled state. In a similar way, the high-field limit corresponds to the situation in which the potential curves associated with the various Zeeman substates are well separated. The condition is $\Omega_B > \Omega_h$, where Ω_h is the last value of Ω_B for which there is a crossing between two potential curves. Therefore, we shall distinguish three domains:

(i) $0 \leqslant \Omega_B \leqslant \Omega_l$ (low magnetic-field regime),
(ii) $\Omega_l \leqslant \Omega_B \leqslant \Omega_h$ (intermediate magnetic-field regime),
(ii) $\Omega_B \geqslant \Omega_h$ (high magnetic-field regime).

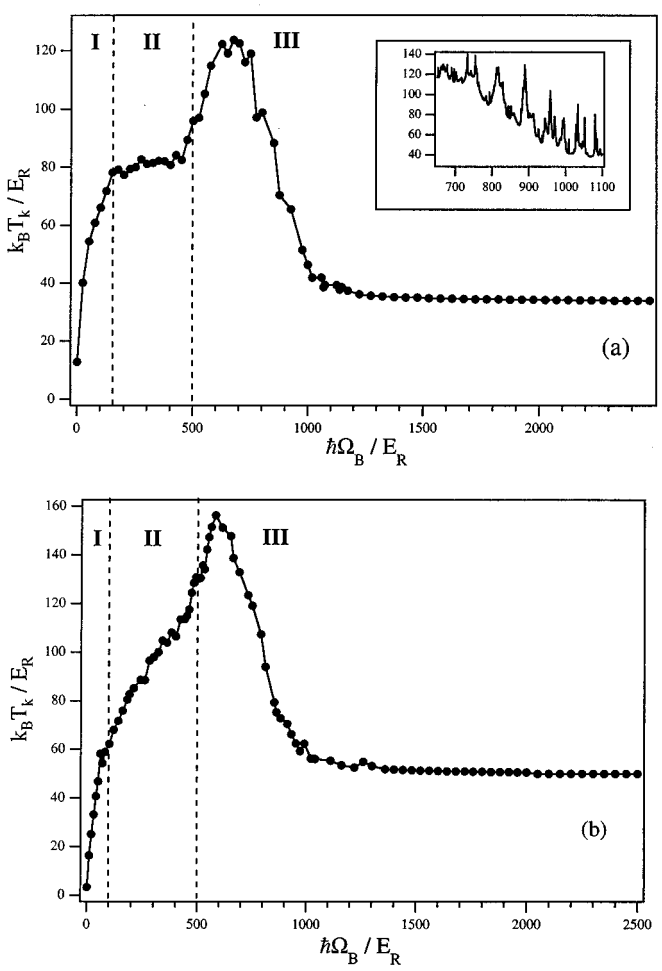

FIG. 1. Temperature dependence of a 1D lin $\perp$ lin gray lattice on the longitudinal magnetic field for two atomic transitions: (a) $J_g=2 \rightarrow J_e=2$; (b) $J_g=2 \rightarrow J_e=1$. The kinetic temperature J_k is related to the rms atomic momentum $p_{\rm rms}$ by $k_B T_k = p_{\rm rms}^2/M$, and Ω_B characterizes the Zeeman shift between the outermost ground-state magnetic sublevels. Both the atomic temperature and the Zeeman shifts are expressed in units of the one-photon recoil energy $E_R=\hbar^2 k^2/2M$ (k being the wave vector of the incident fields). The value of the typical light shift is $\hbar\Delta'=500E_R$. Regions I and III correspond, respectively, to the low- and the high-magnetic-field regimes, where the curves display similar variations of the temperature with Ω_B for both transitions, whereas region II stands for the intermediate-magnetic-field regime, where the temperature variations depend on the atomic transition. The apparent noise on the curves is due to the population resonances [17] originating from the secular approximation used in the band model. Actually, the inset in (a) displays a zoom of the temperature curve, where these resonances appear more clearly. Because most experiments are performed outside the range of validity of the secular approximation, it is expected that one should observe experimentally a smoother variation.

The temperature dependence of these gray lattices on the longitudinal magnetic field can be readily investigated for any transition by using the band method introduced in [4] and employed in [12] for deriving the populations of the lattice energy levels. Typical results for two types of atomic transitions (corresponding to $J_e=J_g$ and $J_e=J_g-1$) are displayed in Figs. 1(a) ($J_g=2 \rightarrow J_e=2$) and 1(b)

($J_g=2\rightarrow J_e=1$), where both the atomic temperature and the Zeeman shifts are expressed in units of the one-photon recoil energy E_R. One clearly sees in these figures that the atomic temperature exhibits the *same* qualitative dependence on the magnetic field, no matter the atomic transition and the associated number of uncoupled states.[1] This dependence, which was observed for all the atomic transitions that we have computed,[2] exhibits several universal features: first, a rapid increase of the atomic temperature in the low magnetic-field regime (i.e., region I of the figures); second, a more gradual increase of temperature for intermediate values of the magnetic field (region II); third, an increase followed by a decrease of the temperature down to an asymptotic value in the high magnetic-field limit (region III). The temperature variation with the magnetic field is always the same in the low and in the high field regimes whatever the atomic transition. It is only in the intermediate field regime that different shapes are observed. For example, one finds a plateau in the case of Fig. 1(a) and a sharp heating in Fig. 1(b). The reason is that region II, previously defined, corresponds to a situation in which there are many crossings between potential curves. The number of crossings and their location depend on the atomic transition (and also on Ω_B), which is why there is no universal behavior for $\Omega_l \leqslant \Omega_B \leqslant \Omega_h$. It is also remarkable to note that the curves of Fig. 1 correspond to that observed by Triché *et al.* [15] in a 3D case. Another output of such numerical calculations is the total magnetization $\langle J_z\rangle/\hbar$ of the lattice. The dependence of this quantity on the magnetic field, represented in Fig. 2 for the cases of a $J_g=2\rightarrow J_e=2$ transition [see Fig. 2(a)] and $J_g=2\rightarrow J_e=1$ transition [see Fig. 2(b)], is also found to be universal in the low and high field regimes. Furthermore, the comparison between Figs. 2 and 1 shows that the atomic magnetization essentially exhibits the same dependence on the magnetic field as the temperature. Starting from a zero value in the absence of magnetic field, it first increases with the magnetic field, reaches a maximum in the intermediate regime (region II), and then decreases down to zero (asymptotic value) in the high-magnetic-field limit (region III). In other words, the lattice behaves either as a paramagnetic or as an antiparamagnetic medium, depending on the magnitude of the magnetic field. Finally, we comment on the apparent scatter of the data in our numerical simulations (Figs. 1 and 2). This phenomenon arises from the coarse-grain sampling of the actual dependences of the magnetization and temperature, which exhibit narrow resonant variations in the secular approximation [17], as shown in the inset in Fig. 1(a). In usual experimental conditions, however, a smoother variation is expected.

We now interpret the results of Figs. 1 and 2. Let us first consider the situation of zero magnetic field. In this case, the atom-laser configuration reminds us of the one employed in 1D subrecoil cooling, and we therefore expect very low atomic temperatures (it is well known, however, that subrecoil temperatures are actually achieved only in the case of a $J_g=1\rightarrow J_e=1$ or $J_g=2\rightarrow J_e=1$ atomic transition). Moreover, the total magnetization of the atoms is then equal to zero for obvious symmetry reasons. Let us now study the influence of the longitudinal magnetic field. As previously mentioned, the situation is particularly simple in the two limiting cases $\Omega_B<\Omega_l$ and $\Omega_B>\Omega_h$. We first consider the low magnetic-field limit, where most atoms accumulate in the energy states associated with the lowest nearly dark optical potentials (we choose for illustration purposes a *positive* magnetic field and a *negative* Zeeman shift). As the magnetic field increases from zero, potential wells of depth $\hbar\Omega_B$ start to develop around points where the uncoupled state coincides with the Zeeman sublevel $m=J_g$ and where atoms become trapped and spatially localized. As a consequence, the total magnetization $\langle J_z\rangle/\hbar$ becomes positive. The fact that the magnetization *increases* with the magnetic field (paramagnetic behavior of the lattice), and eventually corresponds to a significant fraction of J_g [see Fig. 2(a)], results from larger population and spatial localization in the potential

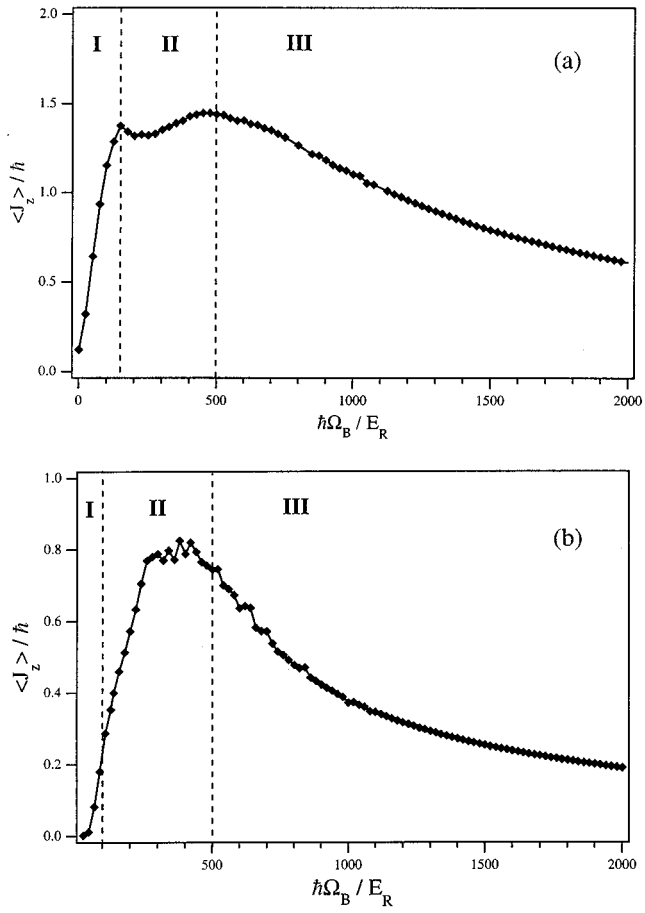

FIG. 2. Variation of the magnetization $\langle J_z\rangle/\hbar$ of the lattice with the magnetic field (the Zeeman splitting is given in recoil units) for the case of a $J_g=2\rightarrow J_e=2$ transition (a) and a $J_g=2\rightarrow J_e=1$ transition (b). The value of the typical light shift is $\hbar\Delta'=500E_R$. The magnetization increases with Ω_B in the low-field limit (region I), corresponding to a *paramagnetic* behavior of the lattice, whereas *antiparamagnetism* appears in the high-magnetic-field limit (region III). This behavior is found for any transition admitting uncoupled states.

[1]A $J_g\rightarrow J_e=J_g$ atomic transition leads to one uncoupled state, whereas a $J_g\rightarrow J_e=J_g-1$ transition involves two nearly dark states.

[2]We have performed numerical calculations for $J_g\rightarrow J_e=J_g$ atomic transitions with angular momenta $1\leqslant J_g\leqslant 4$, and for $J_g\rightarrow J_e=J_g-1$ transitions with $2\leqslant J_g\leqslant 5$.

wells, a phenomenon that also yields higher atomic temperatures.We next consider the high magnetic-field limit, where the lowest and highest optical potentials are associated with the $m=J_g$ and the $m=-J_g$ Zeeman sublevels, respectively, and display alternate potential wells where atoms tend to accumulate.[3] More precisely, the populations of these wells tend *asymptotically* towards the same value because optical pumping eventually populates the $m=-J_g$ wells at points where the light polarization is σ^- with the same efficiency as it populates the $m=J_g$ wells at points where the light is σ^+ polarized. As a consequence, $\langle J_z\rangle/\hbar$ tends to zero, as shown in Fig. 2. The asymptotic behavior of the atomic temperature results from the additional fact that in the limit $\Omega_B \gg \Delta'$, the cooling mechanism due to the Sisyphus effect depends only on the light shift Δ' but not on the Zeeman splitting Ω_B.[4] In fact, when $\Omega_B \gg \Delta'$, apart from the fact that the transitions from $m=J_g$ to $m=-J_g$ may require several optical pumping cycles, the basic properties of the lattice are analogous to those of an optical molasses based on a $J_g=\frac{1}{2}\rightarrow J_e=\frac{1}{2}$ atomic transition [18]. In particular, one expects the asymptotic temperature to be a linear function of Δ' in the limit of large Δ'. This property is illustrated in Fig. 3(a) for $J_g\rightarrow J_e=J_g$ transitions with $1\leqslant J_g\leqslant 4$ and in Fig. 3(b) for $J_g\rightarrow J_e=J_g-1$ transitions with ground-state angular momenta $2\leqslant J_g\leqslant 5$. A remarkable feature presented in these figures is that for a $J_g\rightarrow J_e=J_g-1$ transition the value of the asymptotic temperature is essentially independent of the atomic transition, whereas in the case of a $J_g\rightarrow J_e=J_g$ transition, the slope of the linear part of the curve decreases for increasing values of J_g.

Finally, let us qualitatively describe the beginning of the high magnetic-field regime, corresponding to a Zeeman splitting larger, but of the order of $\hbar\Omega_h$ (see Figs. 1 and 2). In this case, the lowest optical potential still displays potential wells around points associated with σ^+ polarized light and $m=J_g$ internal state, but potential wells having some component on the $m=-J_g$ substate appear in the highest optical potential around points of σ^- polarization. However, because such wells are actually associated with linear superpositions of several substates with relatively large components of Zeeman sublevels different from $m=-J_g$, the departure rate from these wells by optical pumping remains significant, and accordingly their population remains small though nonnegligible. To validate this interpretation, we have calculated the populations in the different optical potentials for increasing values of Ω_B/Δ' and checked that the relative population of $m=-J_g$ in the upper optical potential increases with the magnetic field in the region $\Omega_B>\Omega_h$ but remains smaller than the population of $m=J_g$ in the lowest optical potential.

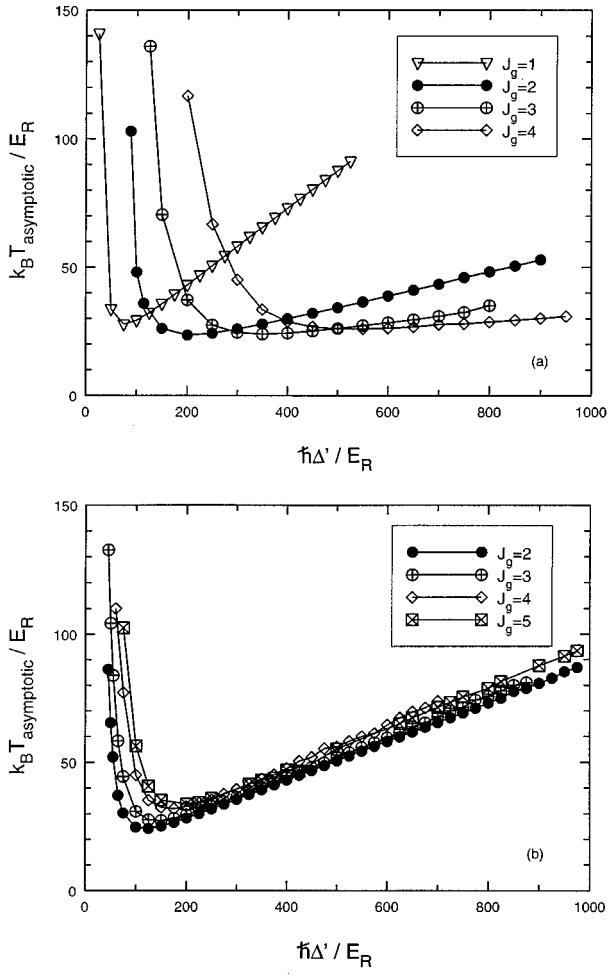

FIG. 3. Variation of the asymptotic temperature in the high-magnetic-field regime with the typical light shift $\hbar\Delta'$ for several atomic transitions: (a) $J_g\rightarrow J_e=J_g$ with $1\leqslant J_g\leqslant 4$; (b) $J_g\rightarrow J_e=J_g-1$ for angular momenta $2\leqslant J_g\leqslant 5$. Both the temperature and the light shift are expressed in units of the one-photon recoil energy. The Zeeman shift between the outermost magnetic sublevels is $\Omega_B=2000E_R$. In the high magnetic-field limit, the cooling mechanism corresponds to a Sisyphus effect between the two outermost ground-state sublevels. As in the conventional Sisyphus cooling mechanism, it leads to a linear dependence of the atomic temperature with $\hbar\Delta'$. A remarkable feature is that the asymptotic temperature is essentially the same for all the transitions of the type $J_g\rightarrow J_e=J_g-1$ that we have calculated. By contrast, the slope of the linear part of the curve decreases with increasing values of J_g in the case of a $J_g\rightarrow J_e=J_g$ transition.

Despite the good qualitative agreement between the previously discussed 1D calculations and the recent observations [15], it is legitimate to wonder whether the 1D model presented here can reliably account for a 3D experimental situation. This problem is of particular importance in the case of gray lattices where significant differences appear in the optical potential topography between the 1D lin$\perp$lin and the 3D stretched tetrahedron geometries, and between $J_e=J_g$ and $J_e=J_g-1$ atomic transitions. We first examine the case of a $J_e\rightarrow J_e=J_g$ transition and discuss two different tetrahedron configurations of the lattice, where two pairs of laser beams propagate in the two orthogonal planes xOz and yOz[16]. In the case where the light beam polarization is or

[3]To verify this point, we have calculated the filling factor of each potential well in the range of large Ω_B. For a $J_g\rightarrow J_e=J_g$ atomic transition, we have found that most of the atoms occupy potential wells associated with the two outermost Zeeman sublevels. In the case of a $J_g\rightarrow J_e=J_g-1$ transition, the situation is more complex and a substantial fraction of the atoms are found in potentials that differ from $|\pm J_g\rangle$ and $|\pm(J_g-1)\rangle$.

[4]We assume that Ω_B and Δ' are much smaller than the frequency detuning.

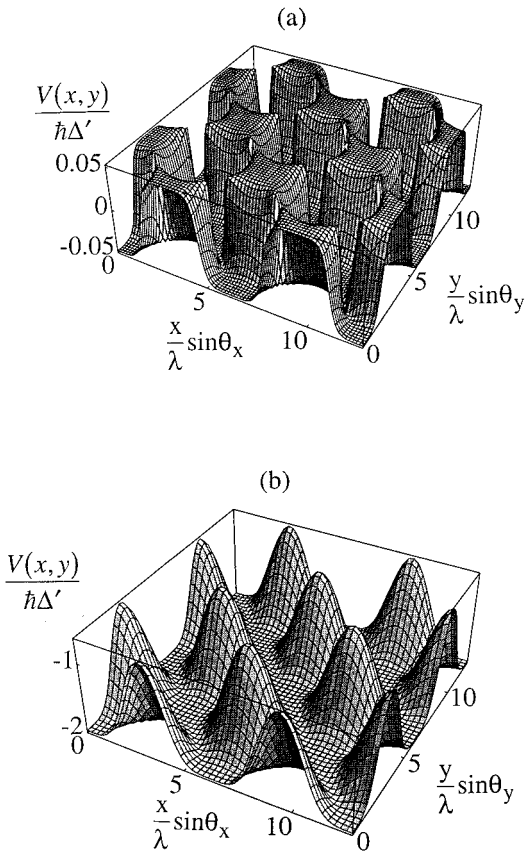

FIG. 4. Three-dimensional gray optical lattices. The section of the lowest optical potential in the xOy plane in the case of a $J_g=2\rightarrow J_e=2$ transition for Zeeman shifts is given by (a) $\Omega_B=0.1\Delta'$ and (b) $\Omega_B=4\Delta'$. The light field configuration is obtained by dividing each beam of the 1D lin $\perp$ lin lattice into two parts, yielding a stretched tetrahedron geometry. The two beams propagating in the xOz plane are linearly polarized along Oy and make an angle $\theta_x=40°$ with Oz. The two counterpropagating beams, linearly polarized along Ox, propagate in the yOz plane, and their propagation directions make an angle $\theta_y=40°$ with the magnetic-field direction ($\perp$ case). In the small magnetic-field regime, the potential valleys are very narrow, preventing atoms from escaping the trapping sites. By contrast, in the high-magnetic-field regime, the potential valleys broaden and the escape rate increases. Note that the optical potentials are expressed in units of the typical light shift $\hbar\Delta'$, and that the space coordinates are given in units of the optical wavelength λ.

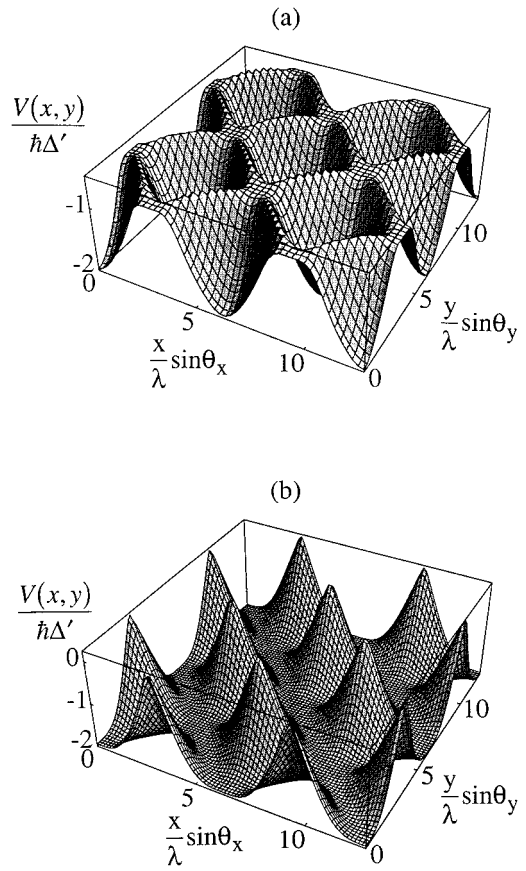

FIG. 5. Three-dimensional gray optical lattices: section of the lowest optical potential in the xOy plane for the $\Omega_B=4\Delta'$, $\theta_x=40°$, and $\theta_y=40°$. The two pairs of light beams are polarized in their propagation planes ($\|$ case). This situation leads to a nonvanishing π component of the light field. (a) Case of a $J_g=2\rightarrow J_e=2$ transition. The π component of light prevents the formation of attractive lines and leads to deep potential wells, which should yield strong spatial localization of the atoms. (b) Case of a $J_g=2\rightarrow J_e=1$ transition. The topography of the optical potential is similar to the one displayed in Fig. 4(b). The optical potentials are expressed in units of the typical light shift $\hbar\Delta'$, and the space coordinates are given in units of the optical wavelength λ.

thogonal to the propagation planes ($\perp$ configuration of [13]), the total laser field displays diagonal lines of constant circular polarization in the xOy plane. In the presence of a longitudinal magnetic field, these lines are therefore associated with minima of the optical potential and atoms can escape from a confining site by following these lines. It thus appears that this tetrahedron geometry differs from the 1D lin $\perp$ lin configuration by the fact that the 1D lattice of optical potential *wells* has been substituted for a network of *attractive lines* corresponding to the eigenstates $m=\pm J_g$. However, in the limit of small values of Ω_B, where the associated potential valleys in the xOy plane are extremely narrow [Fig. 4(a)], one can consider that atoms located in trapping sites are *almost* confined in three dimensions, and one expects the temperature dependence on the magnetic field to be basically the same as in 1D lin $\perp$ lin gray lattices. As the magnetic field increases, however, the potential valleys broaden and the probability for atoms to escape along these lines becomes more important [Fig. 4(b)]. In fact, this phenomenon is not expected to yield significant differences in the lattice temperature because of the optical pumping processes undergone by the escaping atoms due to the transverse extension of their wave function.[5] Consequently, it is most likely that the mechanisms responsible for the increase and decrease of the atomic temperature described above keep their relevance in this 3D geometry.

Consider now the situation in which the light beams are polarized in their propagation planes ($\|$ configuration of

[5]This mechanism essentially occurs between the lowest and highest potential surfaces that exhibit a spatial modulation along these lines.

[13]). In that case, the total electric field exhibits a nonvanishing space-dependent π component, which yields a spatial modulation of the optical potentials in any direction. In particular, the lowest potential surface in the xOy plane exhibits genuine potential wells, which should lead to a strong 3D confinement of the atoms [see Fig. 5(a)] on a large range of magnetic field. The deep analogy between this configuration and the previously discussed 1D lin $\perp$ lin situation suggests that they should share the same basic physical properties. Finally, we discuss the case of a $J_g \rightarrow J_e = J_g - 1$ atomic transition for the same tetrahedron configurations of the light field. In the case in which the light beams have a polarization orthogonal to the propagation plane, the lowest optical potential essentially exhibits the same topography as in the case of a $J_g \rightarrow J_e = J_g$ transition, hence a similar physical behavior is expected. The absence of genuine optical potential wells is *also* found in the situation in which the light beams are polarized in their propagation planes [Fig. 5(b)]. This is due to the fact that $J_g \rightarrow J_e = J_g - 1$ atomic transitions admit one set of attractive lines which is insensitive to the π component of the light polarization.

In conclusion, we have investigated the dependence of the temperature and of the magnetization of 1D lin $\perp$ lin gray optical lattices on the longitudinal magnetic field in the cases of $J \rightarrow J$ and $J \rightarrow J-1$ atomic transitions, and found the same behavior for both quantities independently of the value of J. It is legitimate to wonder whether the same behavior occurs for a lin $\perp$ lin ''bright'' lattice based on a $J \rightarrow J+1$ transition. We have calculated the variation of the temperature and of the magnetization of such a lattice versus Ω_B in the case of a $J_g = 1 \rightarrow J_e = 2$ transition and found essentially the same dependences. However, it is important to note that the underlying physical mechanisms are very different in bright optical lattices. When $\Omega_B = 0$, there are indeed two kinds of wells in the lowest optical potential, which are essentially associated with the magnetic sublevels $m = 1$ and $m = -1$. As Ω_B increases, these potential wells acquire different depths and exchange populations, leading to a paramagnetic behavior of the lattice that was recently demonstrated experimentally [19]. As the magnetic field increases, one kind of potential wells vanishes, reducing the Sisyphus cooling efficiency. The situation simplifies in the limit $\Omega_B > \Omega_h$, where it becomes basically identical to the high magnetic-field regime discussed here: potential wells appear on the optical potentials associated with the Zeeman sublevels $m = 1$ and $m = -1$, which asymptotically become equally populated. The main difference with gray lattices is that these potential wells correspond to a *maximum* interaction with light. In principle, the same argument could be applied to higher J's, but the computation is more difficult using the band method because of the population resonances mentioned above [17]. Note, however, that the experimental demonstration of such a behavior for a high J value may present some difficulties because of the very long optical pumping times between the Zeeman sublevels $m = J$ and $m = -J$, which may reduce the velocity capture range of the lattice.

The authors thank C. Triché for helpful discussions. The work was supported in part by the EEC and NEDO (Japan). Laboratoire Kastler-Brossel is an unité de recherche de l'ENS et de l'Université Pierre et Marie Curie associeé au CNRS.

[1] T. W. Hänsch and A. Schawlow, Opt. Commun. **13**, 68 (1975).
[2] P. Lett *et al.*, Phys. Rev. Lett. **61**, 169 (1988).
[3] J. Dalibard and C. Cohen-Tannoudji, J. Opt. Soc. Am. B **6**, 2023 (1989); P. J. Ungar *et al.*, *ibid.* **6**, 2058 (1989).
[4] Y. Castin and J. Dalibard, Europhys. Lett. **14** (8), 761 (1991).
[5] J.-Y. Courtois and G. Grynberg, Phys. Rev. A **46**, 7060 (1992).
[6] P. Verkerk *et al.*, Phys. Rev. Lett. **68**, 3861 (1992).
[7] P. Jessen *et al.*, Phys. Rev. Lett. **69**, 49 (1992).
[8] A. Hemmerich and T. W. Hänsch, Phys. Rev. Lett. **70**, 410 (1993).
[9] G. Grynberg *et al.*, Phys. Rev. Lett. **70**, 2249 (1993); P. Verkerk *et al.*, Europhys. Lett. **26**, 171 (1994).
[10] A. Hemmerich, C. Zimmerman, and T. W. Hänsch, Europhys. Lett. **22**, 89 (1994).
[11] A. Kastberg *et al.*, Phys. Rev. Lett. **74**, 1542 (1995).
[12] G. Grynberg and J.-Y. Courtois, Europhys. Lett. **27**, 41 (1994).
[13] D. Boiron *et al.*, Phys. Rev. A **52**, 3425 (1995).
[14] A. Hemmerich *et al.*, Phys. Rev. Lett. **75**, 37 (1995); J. Guo and J. Cooper, Phys. Rev. A **52**, R1819 (1995).
[15] C. Triché *et al.*, Opt. Commun. (to be published).
[16] K. I. Petsas, A. B. Coates, and G. Grynberg, Phys. Rev. A **50**, 5173 (1994).
[17] In the secular approximation, the optical pumping rate should be smaller than $E_R/\hbar$; see J.-Y. Courtois, Ann. Phys. (Paris) (to be published).
[18] J. Guo and P. R. Berman, Phys. Rev. A **48**, 3225 (1993).
[19] D. R. Meacher *et al.*, Phys. Rev. Lett. **74**, 1958 (1995).